Electronic Supplementary Information (ESI)

Solution-processable organic light-emitting diodes utilizing electroluminescent perylene tetraester-based columnar liquid crystals

Shallu Dhingra,[a] Iram Siddiqui,[b] Santosh Prasad Gupta,[c] Shahnawaz,[b] Jayachandran Jayakumar,[b] Jwo-Huei Jou*[b] and Santanu Kumar Pal*[a]

[a]*Department of Chemical Sciences, Indian Institute of Science Education and Research (IISER) Mohali, Sector-81, SAS Nagar, Knowledge City, Manauli-140306, India. E-mail: skpal@iisermohali.ac.in, santanupal.20@gmail.com*
[b]*Department of Materials Science and Engineering, National Tsing Hua University, Hsinchu 30013, Taiwan, E-mail: jjou@mx.nthu.edu.tw*
[c]*Department of Physics, Patna University, Patna-800005, India*

1. Materials and instrumentation details

1.1. Materials. All commercially available solvents and chemicals (AR quality) were used as such to carry out the reactions without further purification or modification. Silica gel (100–200 mesh) and neutral alumina were used for the column chromatography to purify the final compounds and intermediates. For thin-layer chromatography (TLC), aluminum sheets pre-coated with silica gel (Merck, Kieselgel 60, F254) were used.

1.2. Instrumentation

The instrumental details are similar, as reported in our earlier work.[1-4]

2. Experimental Section

The reaction scheme to synthesize the final compounds **1a-c** is below:

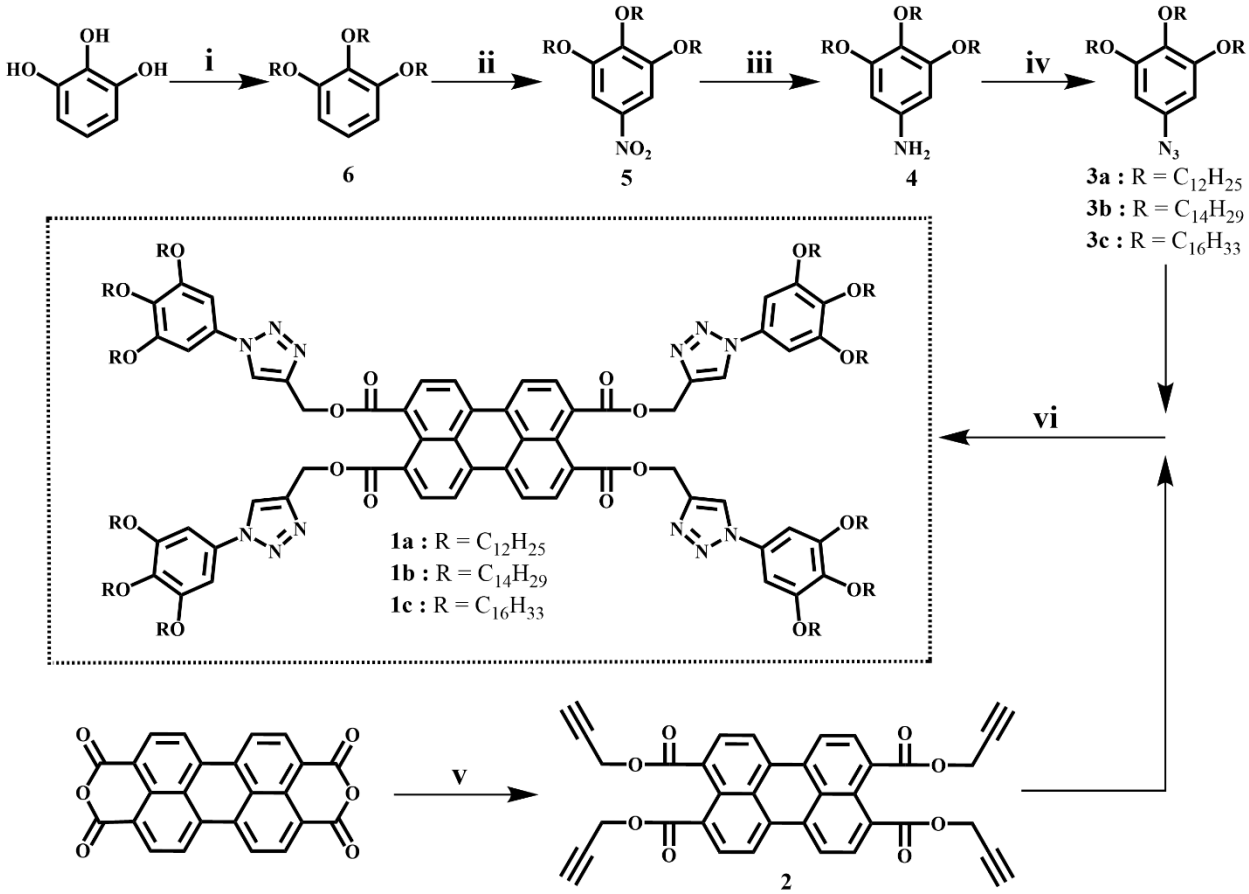

Scheme S1. Reagents and Conditions: (i) K_2CO_3, alkyl bromide, dimethylformamide, reflux, 72 h, yield - **6a**: 74%, **6b**: 75%, **6c**: 78%; (ii) $NaNO_2$, conc. HNO_3, DCM, RT, 12 h, yield - **5a**: 68%,

5b: 65%, **5c**: 67%; (iii) Pd/C, H_2 filled balloon, dry THF, 12 h, yield - **4a**: 90%, **4b**: 89%, **4c**: 92%; (iv) TMS-azide, *tert*-butyl nitrite, ACN, RT, 12 h, yield - **3a**: 72%, **3b**: 74%, **3c**: 75 %; (v) i. KOH, H_2O, 100 °C, 1 h; ii. propargyl bromide, tetraoctylammonium bromide (TOABr), 100 °C, 24 h, yield - 40%; (vi) Sodium ascorbate, $CuSO_4 \cdot 5H_2O$, $H_2O/EtOH/CHCl_3$ (1:1:2), 65 °C, 48 h, yield - **1a**: 53%, **1b**: 56%, **1c**: 57%.

Synthesis. For the preparation of compounds **2**, **4**, **5**, and **6**, the same synthetic pathway was used as previously.[1,5]

This present work reports the synthesis of final compounds **1a-c** and intermediates **3a-c**.

2.1. General procedure for the synthesis of 5-azido-1,2,3-tris(alkoxy)benzene (3a-c)

The synthetic pathway followed is the same as reported elsewhere, with slight modification.[6]

Compound **4** (500 mg, 1 equiv.) was dissolved in a dried 1:1 (v/v) mixture of acetonitrile (2 mL) and tetrahydrofuran (THF) (2.2 mL). After cooling the solution to 0 °C, *tert*-butyl nitrite (1.1 equiv.) was dropwise added to the reaction mixture, followed by the gradual addition of trimethylsilyl azide (1.8 equiv.). The reaction was kept for stirring at room temperature (RT) for 12 h. The extraction of crude product was done using dichloromethane (DCM) and water mixture. For purification, column chromatography (Silica Gel 100-200 mesh) with ethyl acetate/hexane (10:90) as eluent was used to give **3** as a brown solid. Yield - **3a**: 72%, **3b**: 74%, **3c**: 75%.

5-azido-1,2,3-tris(dodecyloxy)benzene (**3a**)

^{1}H NMR (400 MHz, $CDCl_3$, δ in ppm): δ 6.21 (s, 2H, Ar), δ 3.95-3.88 (m, 6H, 3 × OCH_2), δ 1.82-1.68 (m, 6H, 3 × CH_2), δ 1.48-1.42 (m, 6H, 3 × CH_2), δ 1.33-1.26 (m, 48H, alkyl protons), δ 0.88 (t, 9H, 3 × CH_3).

^{13}C NMR (100 MHz, $CDCl_3$, δ in ppm): δ 153.93, 135.45, 134.98, 97.66, 73.58, 69.17, 31.96, 31.95, 30.29, 29.77, 29.72, 29.68, 29.65, 29.63, 29.40, 29.29, 26.14, 26.07, 22.72, 14.13.

IR (ATR, cm^{-1}): 2921, 2852, 2107, 1591, 1500, 1464, 1440, 1380, 1254, 1231, 1117, 1013, 967, 810, 722, 609, 514, 490, 479, 472, 460, 447, 438, 420.

5-azido-1,2,3-tris(tetradecyloxy)benzene (**3b**)

^{1}H NMR (400 MHz, $CDCl_3$, δ in ppm): *δ* 6.20 (s, 2H, Ar), *δ* 3.95-3.88 (m, 6H, 3 × OCH_2), *δ* 1.82-1.70 (m, 6H, 3 × CH_2), *δ* 1.47-1.42 (m, 6H, 3 × CH_2), *δ* 1.30-1.26 (m, 60H, alkyl protons), *δ* 0.88 (t, 9H, 3 × CH_3).

^{13}C NMR (100 MHz, $CDCl_3$, δ in ppm): *δ* 153.92, 135.42, 134.98, 97.63, 73.58, 69.16, 31.96, 30.30, 29.78, 29.74, 29.70, 29.66, 29.63, 29.41, 29.29, 26.15, 26.07, 22.73, 14.15.

IR (ATR, cm^{-1}): 2917, 2850, 2107, 1587, 1505, 1466, 1440, 1383, 1261, 1233, 1123, 988, 969, 801, 738, 607, 515, 491, 478, 472, 461, 437, 425, 416.

5-azido-1,2,3-tris(hexadecyloxy)benzene (**3c**)

^{1}H NMR (400 MHz, $CDCl_3$, δ in ppm): *δ* 6.21 (s, 2 H, Ar), *δ* 3.95-3.88 (m, 6H, 3 × OCH_2), *δ* 1.82-1.68 (m, 6 H, 3 × CH_2), *δ* 1.49-1.42 (m, 6 H, 3 × CH_2), *δ* 1.30-1.26 (m, 72 H, alkyl protons), *δ* 0.88 (t, 9H, 3 × CH_3).

^{13}C NMR (100 MHz, $CDCl_3$, δ in ppm): *δ* 153.94, 135.48, 135.00, 97.67, 73.56, 69.16, 31.97, 30.31, 29.78, 29.75, 29.71, 29.67, 29.64, 29.42, 29.31, 26.16, 26.08, 22.72, 14.13.

IR (ATR, cm^{-1}): 2917, 2850, 2108, 1590, 1504, 1467, 1440, 1383, 1260, 1230, 1123, 987, 802, 740, 722, 515, 491, 479, 456, 438, 427, 416.

2.2. Procedure for synthesis of tetrakis((1-(3,4,5-tris(dodecyloxy)phenyl)-1H-1,2,3-triazol-4-yl)methyl) perylene-3,4,9,10-tetracarboxylate (1a)

The synthetic pathway followed is the same as reported elsewhere, with slight modification.[7]

Tetra(prop-2-yn-1-yl) perylene-3,4,9,10-tetracarboxylate (**2**) (50 mg, 1 equiv.), 5-azido-1,2,3-tris(dodecyloxy)benzene (**3a**) (463.08 mg, 8 equiv.), $CuSO_4{\cdot}5H_2O$ (21.50 mg, 1 equiv.) and sodium ascorbate (10.24 mg, 0.6 equiv.) were dissolved in the solvent mixture of $CHCl_3$ (4 ml)/EtOH (2 ml)/H_2O (2 ml). The reaction mixture was stirred vigorously and refluxed at 65 °C for 48 h. The crude product was extracted using chloroform ($CHCl_3$), followed by the purification using column chromatography (neutral alumina, ethyl acetate/hexane 15:85) to give a yellow solid after recrystallization using MeOH/DCM. Yield - 53%.

^{1}H NMR (400 MHz, $CDCl_3$, δ in ppm): *δ* 8.35-8.33 (d, 4H, *J* = 8.00 Hz), *δ* 8.16 (s, 4H), *δ* 8.15-8.13 (d, 4H, *J* = 8.00 Hz), *δ* 6.89 (s, 8H), *δ* 5.50 (s, 8H), *δ* 3.99-3.94 (m, 24H), *δ* 1.83-1.70 (m, 24H), *δ* 1.49-1.41 (m, 24H), *δ* 1.32-1.24 (m, 192H), *δ* 0.89-0.85 (m, 36H).

^{13}C NMR (100 MHz, $CDCl_3$, δ in ppm): *δ* 168.19, 153.78, 142.86, 138.38, 133.28, 132.26, 131.16, 129.43, 129.05, 128.75, 122.92, 121.71, 99.41, 73.63, 69.41, 58.76, 31.97, 31.95, 30.35, 29.80, 29.78, 29.74, 29.69, 29.67, 29.65, 29.44, 29.40, 29.29, 26.14, 26.10, 22.72, 14.15.

IR (ATR, cm^{-1}): 2922, 2853, 1717, 1598, 1508, 1460, 1384, 1267, 1231, 1158, 1115, 1072, 1047, 1018, 824, 721, 486.

Elemental analysis (%): Calculated: C 74.96, H 10.11, N 5.14. Found: C 74.50, H 10.36, N 5.04.

2.3. Procedure for synthesis of tetrakis((1-(3,4,5-tris(tetradecyloxy)phenyl)-1H-1,2,3-triazol-4-yl)methyl) perylene-3,4,9,10-tetracarboxylate (1b)

The procedure used is the same as used for synthesizing **1a**, using 5-azido-1,2,3-tris(tetradecyloxy)benzene (**3b**) to give the final product **1b** as yellow solid after recrystallization using MeOH/DCM. Yield - 56%.

^{1}H NMR (400 MHz, $CDCl_3$, δ in ppm): *δ* 8.35-8.33 (d, 4H, *J* = 8.00 Hz), *δ* 8.16 (s, 4H), *δ* 8.15-8.13 (d, 4H, *J* = 8.00 Hz), *δ* 6.89 (s, 8H), *δ* 5.50 (s, 8H), *δ* 3.99-3.94 (m, 24H), *δ* 1.83-1.70 (m, 24H), *δ* 1.48-1.41 (m, 24H), *δ* 1.27-1.24 (m, 240H), *δ* 0.88-0.85 (m, 36H).

^{13}C NMR (100 MHz, $CDCl_3$, δ in ppm): *δ* 168.20, 153.78, 142.86, 138.38, 133.39, 132.26, 131.20, 129.47, 129.05, 128.78, 122.91, 121.74, 99.40, 73.64, 69.41, 58.78, 31.96, 30.35, 29.80, 29.75, 29.71, 29.68, 29.65, 29.45, 29.43, 29.41, 29.30, 26.15, 26.10, 22.73, 14.16.

IR (ATR, cm^{-1}): 2922, 2852, 1718, 1599, 1508, 1461, 1384, 1267, 1231, 1158, 1116, 1072, 1047, 1019, 825, 735, 704, 491.

Elemental analysis (%): Calculated: C 75.95, H 10.51, N 4.66. Found: C 75.75, H 10.68, N 4.53.

2.4. Procedure for synthesis of tetrakis((1-(3,4,5-tris(hexadecyloxy)phenyl)-1H-1,2,3-triazol-4-yl)methyl) perylene-3,4,9,10-tetracarboxylate (1c)

The procedure used is the same as for the synthesis of **1a**, using 5-azido-1,2,3-tris(hexadecyloxy)benzene (**3c**) to give the final product **1c** as yellow solid after recrystallization using MeOH/DCM. Yield - 57%.

^{1}H NMR (400 MHz, $CDCl_3$, δ in ppm): *δ* 8.34-8.32 (d, 4H, *J* = 8.00 Hz), *δ* 8.17 (s, 4H), *δ* 8.14-8.12 (d, 4H, *J* = 8.00 Hz), *δ* 6.89 (s, 8H), *δ* 5.50 (s, 8H), *δ* 3.99-3.93 (m, 24H), *δ* 1.83-1.70 (m, 24H), *δ* 1.49-1.41 (m, 24H), *δ* 1.30-1.24 (m, 288H), *δ* 0.88-0.85 (m, 36H).

^{13}C NMR (100 MHz, $CDCl_3$, δ in ppm): δ 168.18, 153.79, 142.86, 138.39, 133.32, 132.26, 131.18, 129.45, 129.08, 128.78, 122.91, 121.72, 99.41, 73.63, 69.41, 58.77, 31.96, 30.36, 29.80, 29.76, 29.70, 29.69, 29.66, 29.46, 29.41, 29.30, 26.15, 26.10, 22.73, 14.15.

IR (ATR, cm^{-1}): 2919, 2851, 1719, 1599, 1509, 1463, 1384, 1270, 1232, 1159, 1118, 1071, 1047, 1019, 825, 722, 486.

Elemental analysis (%): Calculated: C 76.78, H 10.84, N 4.26. Found: C 76.35, H 10.70, N 4.10.

3. NMR Spectra

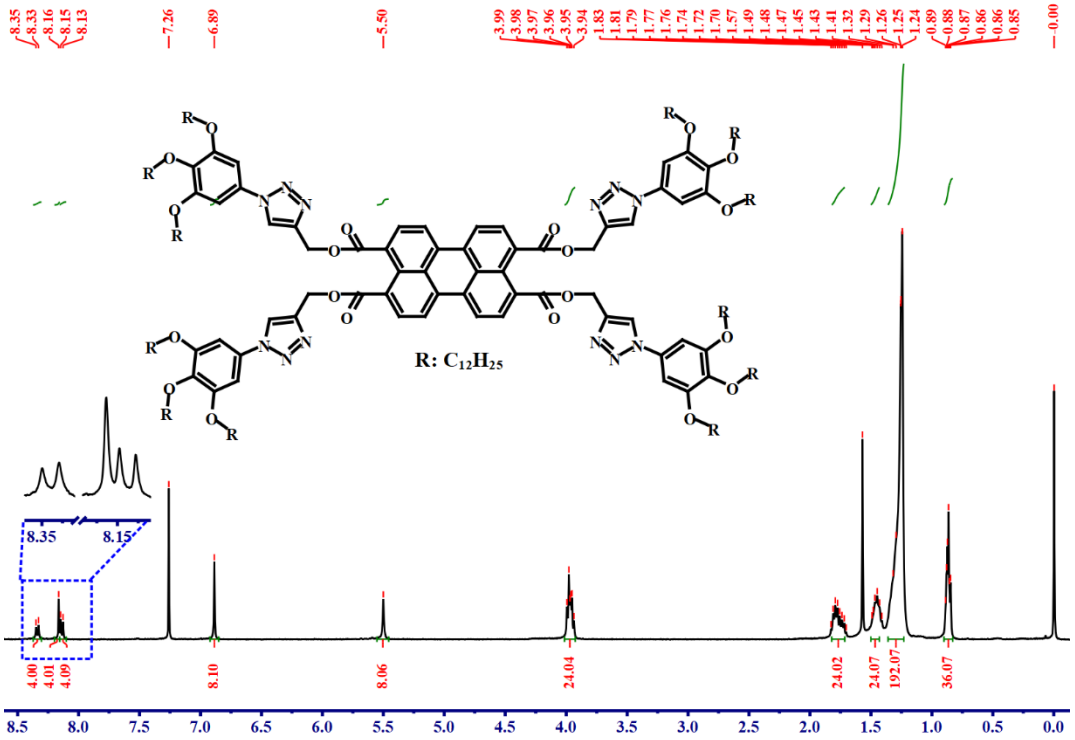

Figure S1. ^{1}H NMR spectrum of compound **1a**.

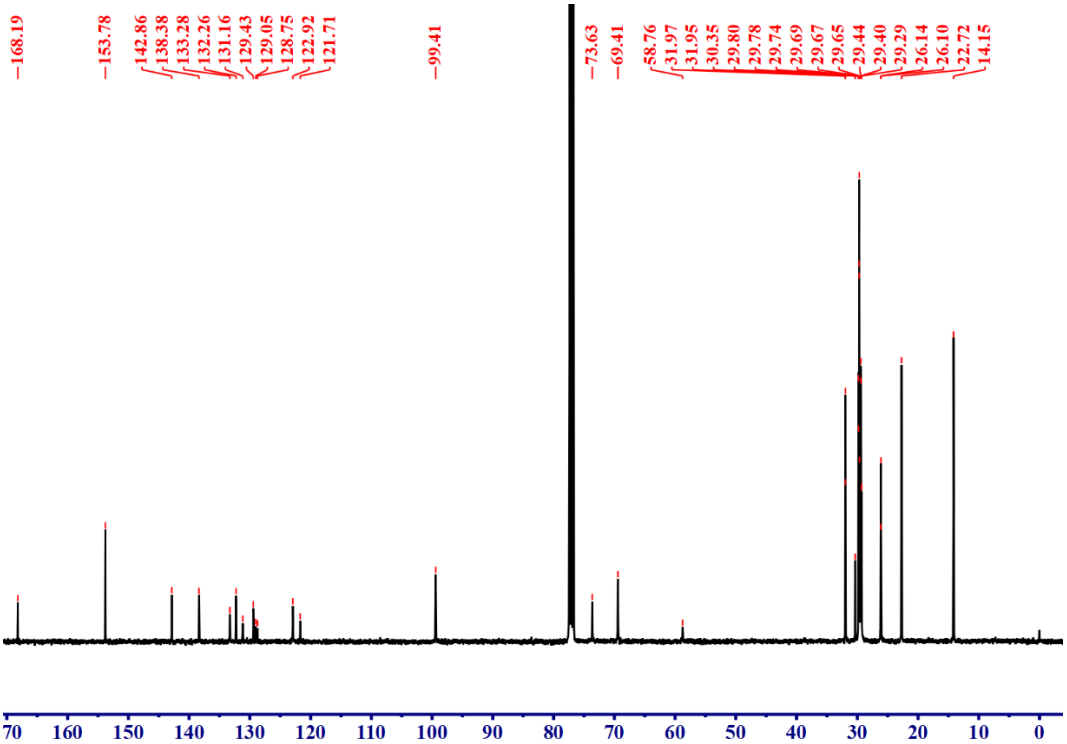

Figure S2. ^{13}C NMR spectrum of compound **1a**.

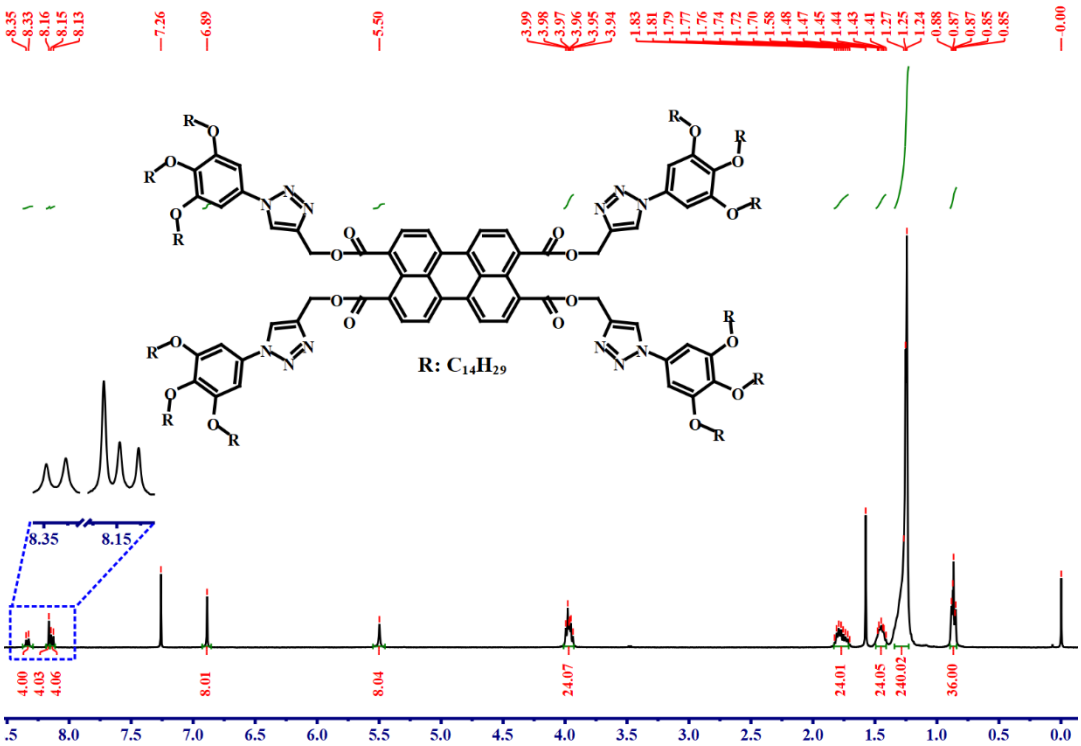

Figure S3. ^{1}H NMR spectrum of compound **1b**.

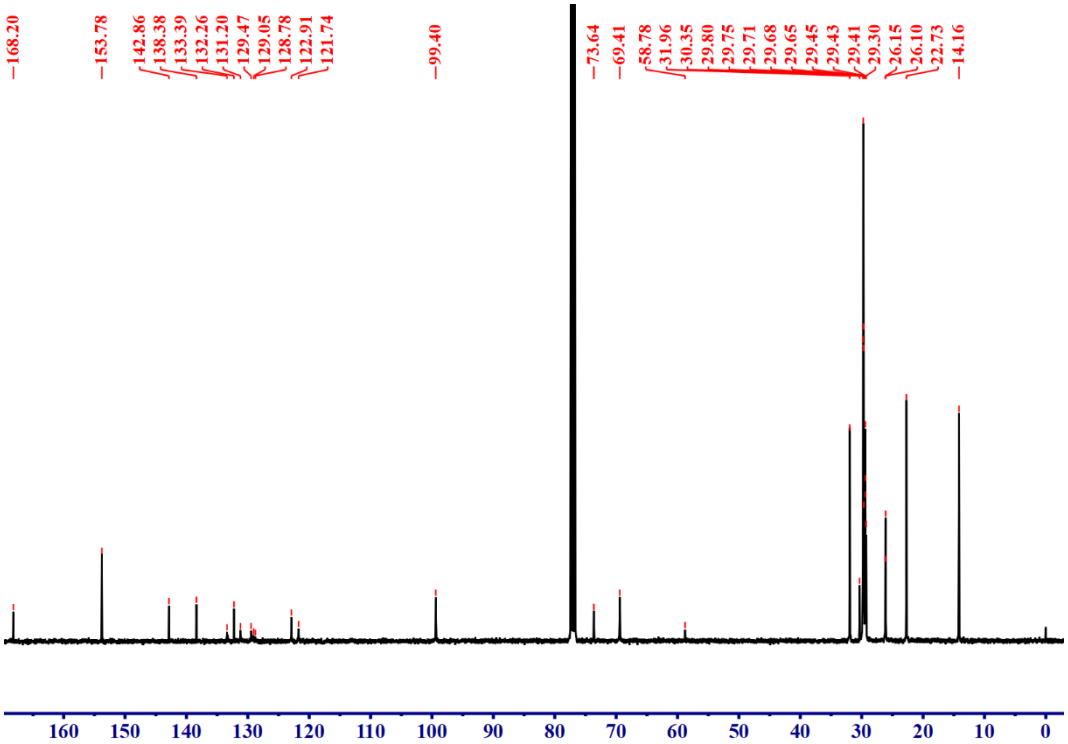

Figure S4. ^{13}C NMR spectrum of compound **1b**.

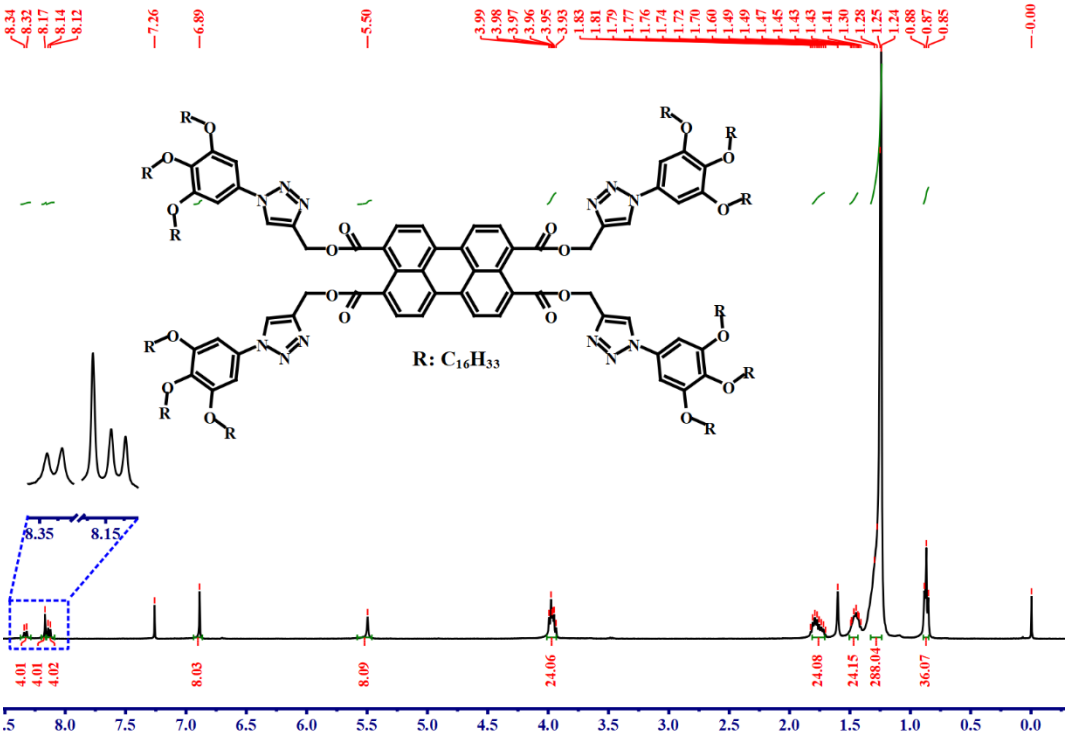

Figure S5. ^{1}H NMR spectrum of compound **1c**.

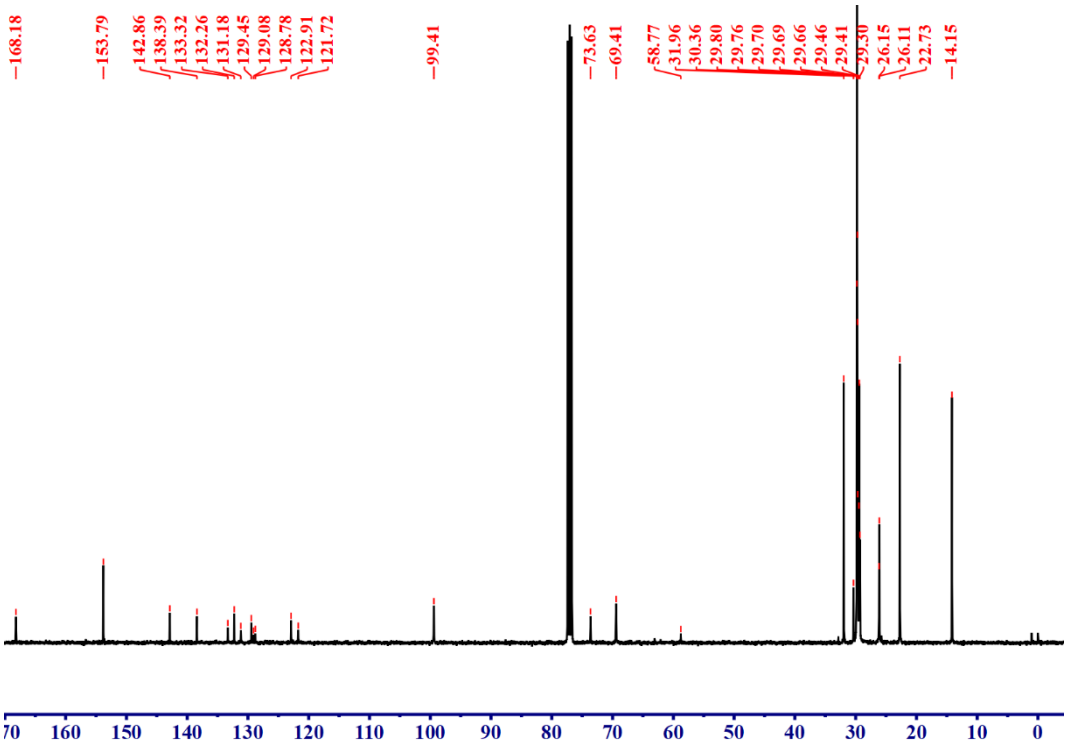

Figure S6. ^{13}C NMR spectrum of compound **1c**.

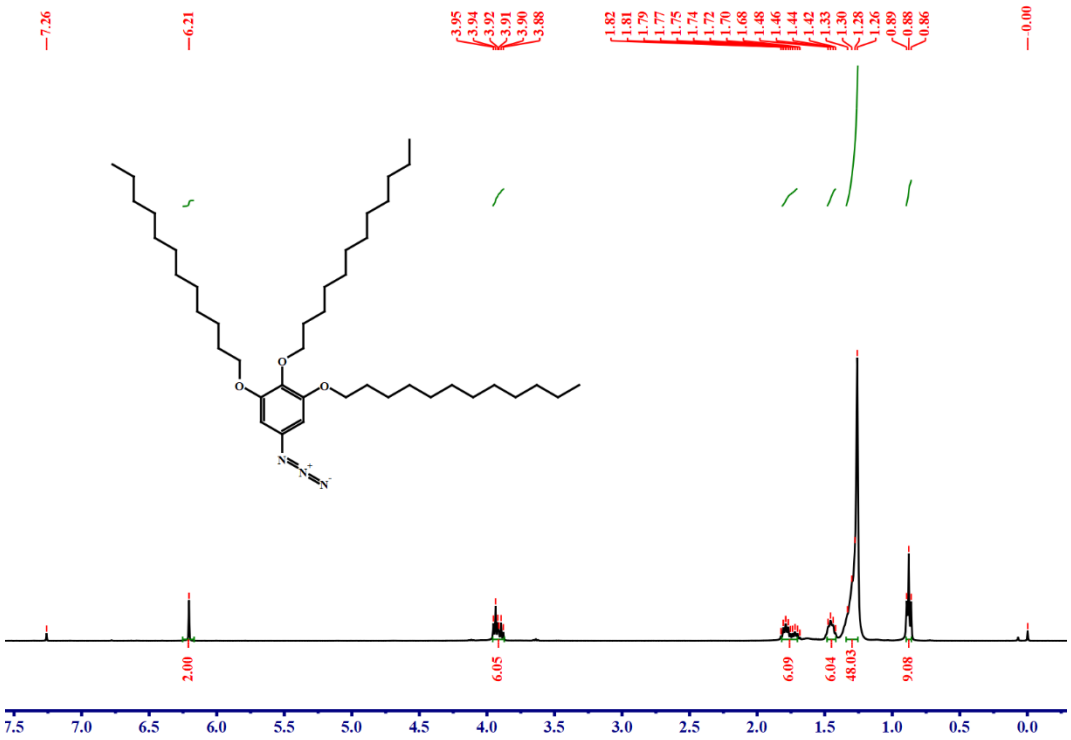

Figure S7. ^{1}H NMR spectrum of compound **3a**.

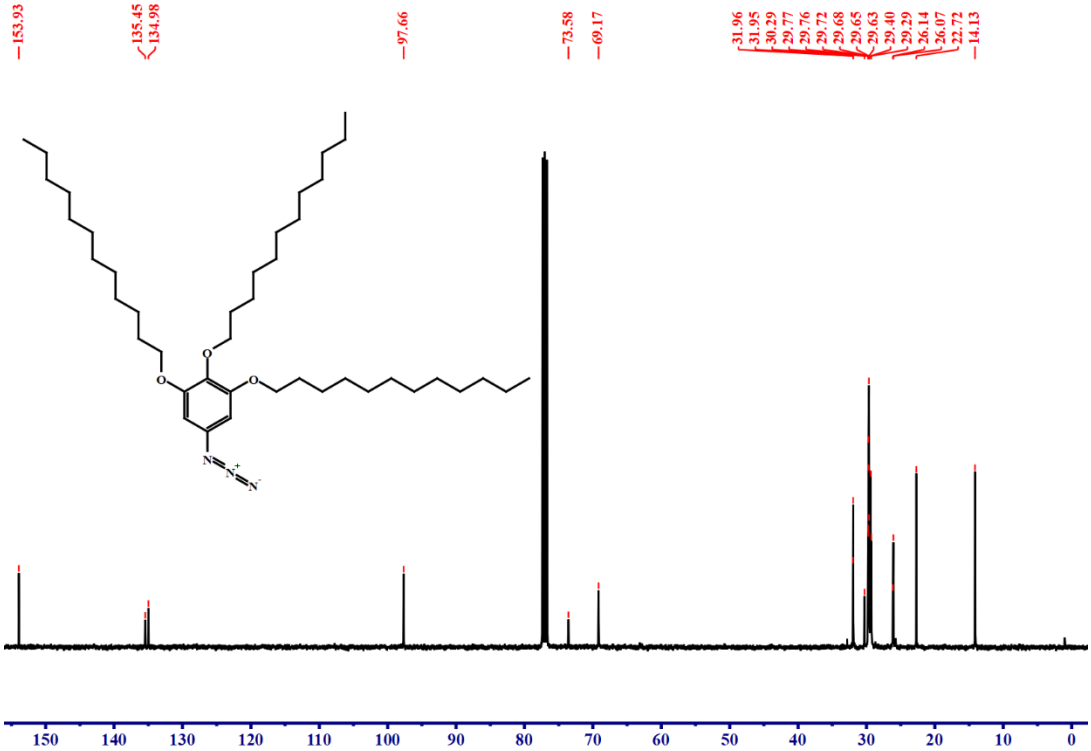

Figure S8. ^{13}C NMR spectrum of compound **3a**.

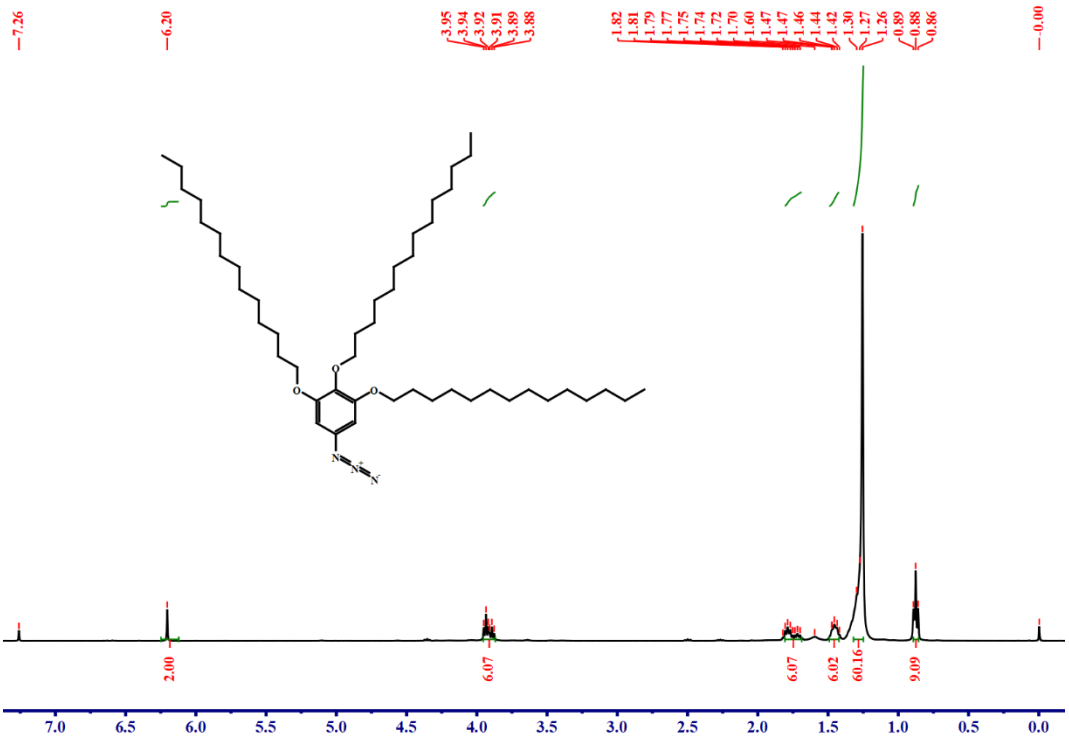

Figure S9. ^{1}H NMR spectrum of compound **3b**.

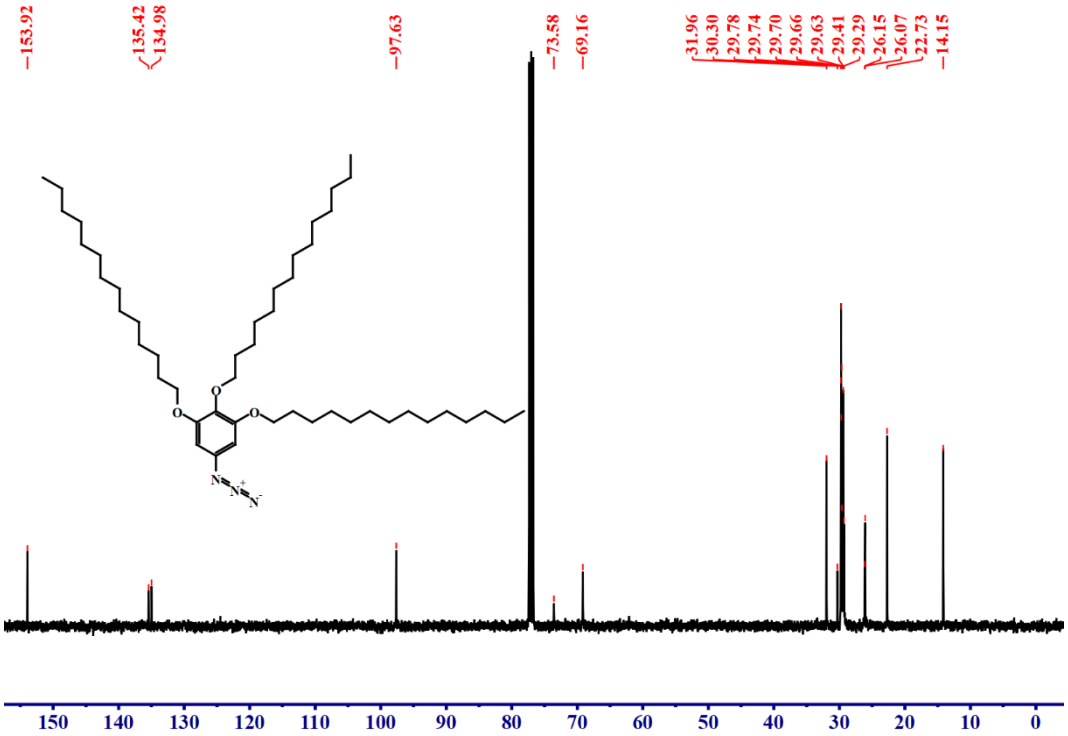

Figure S10. ^{13}C NMR spectrum of compound **3b**.

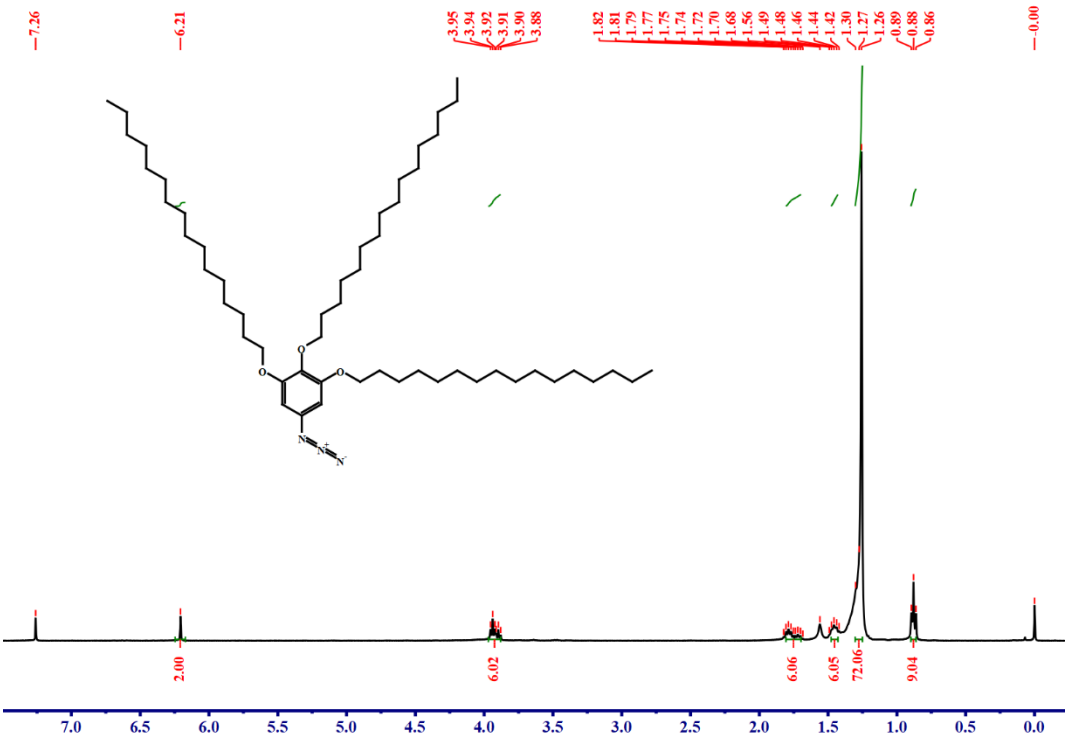

Figure S11. ^{1}H NMR spectrum of compound **3c**.

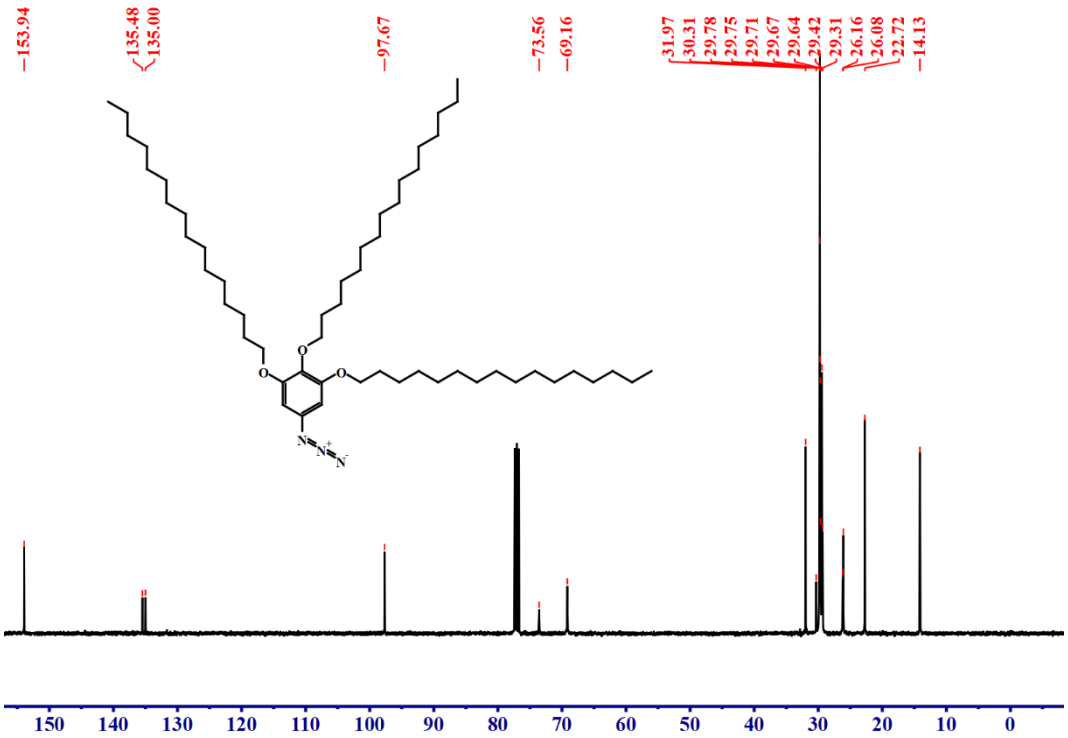

Figure S12. ^{13}C NMR spectrum of compound **3c**.

4. Polarized Optical Microscopic (POM) Images

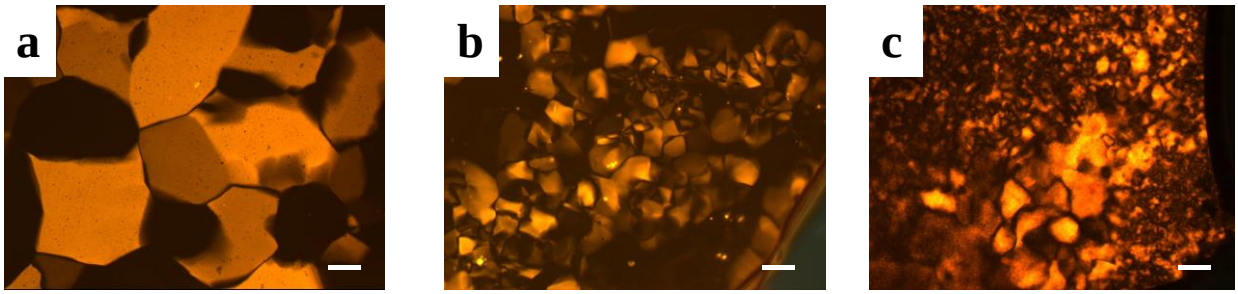

Figure S13. Textures of (a) compound **1a** at 23.4 ℃, (b) compound **1b** at 26.8 ℃, (c) compound **1c** at 40.1 ℃ obtained on cooling under crossed polarizers using X100 magnification. The scale bar is 40 µm.

5. Differential Scanning Calorimetry (DSC) Thermogram

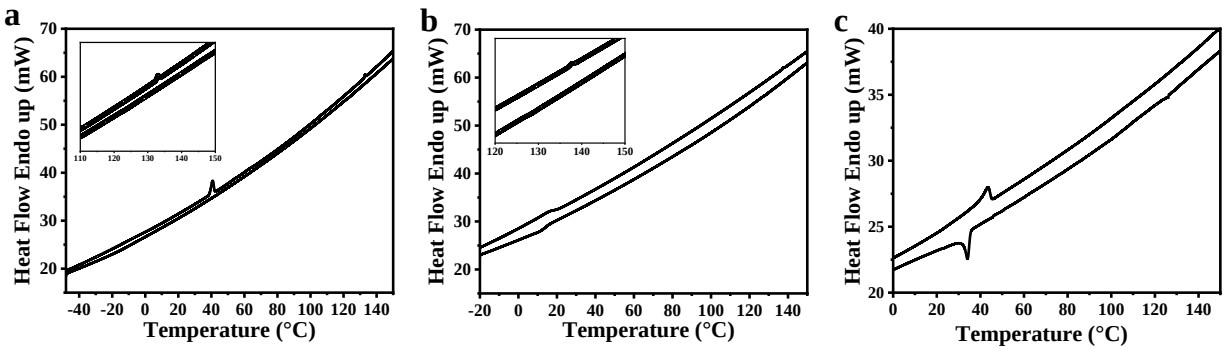

Figure S14. DSC thermogram obtained with 5 ℃/min heating and cooling rates for compounds (a) **1a**, (b) **1b**, and (c) **1c** under a nitrogen atmosphere.

6. Thermogravimetric Analysis (TGA) Curve

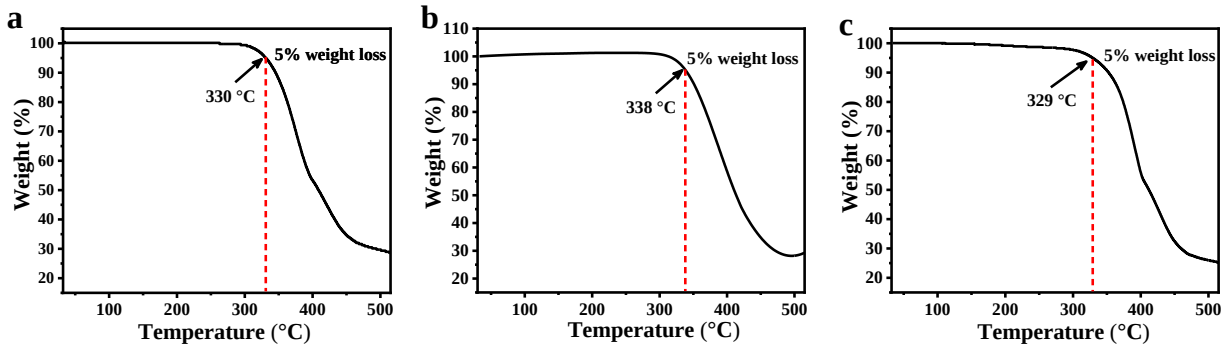

Figure S15. TGA curves recorded with a 10 °C/min heating rate for compounds (a) **1a**, (b) **1b**, and (c) **1c** under a nitrogen atmosphere. Temperatures corresponding to 5% weight loss are shown in the figure.

7. X-ray Diffraction (XRD) Studies

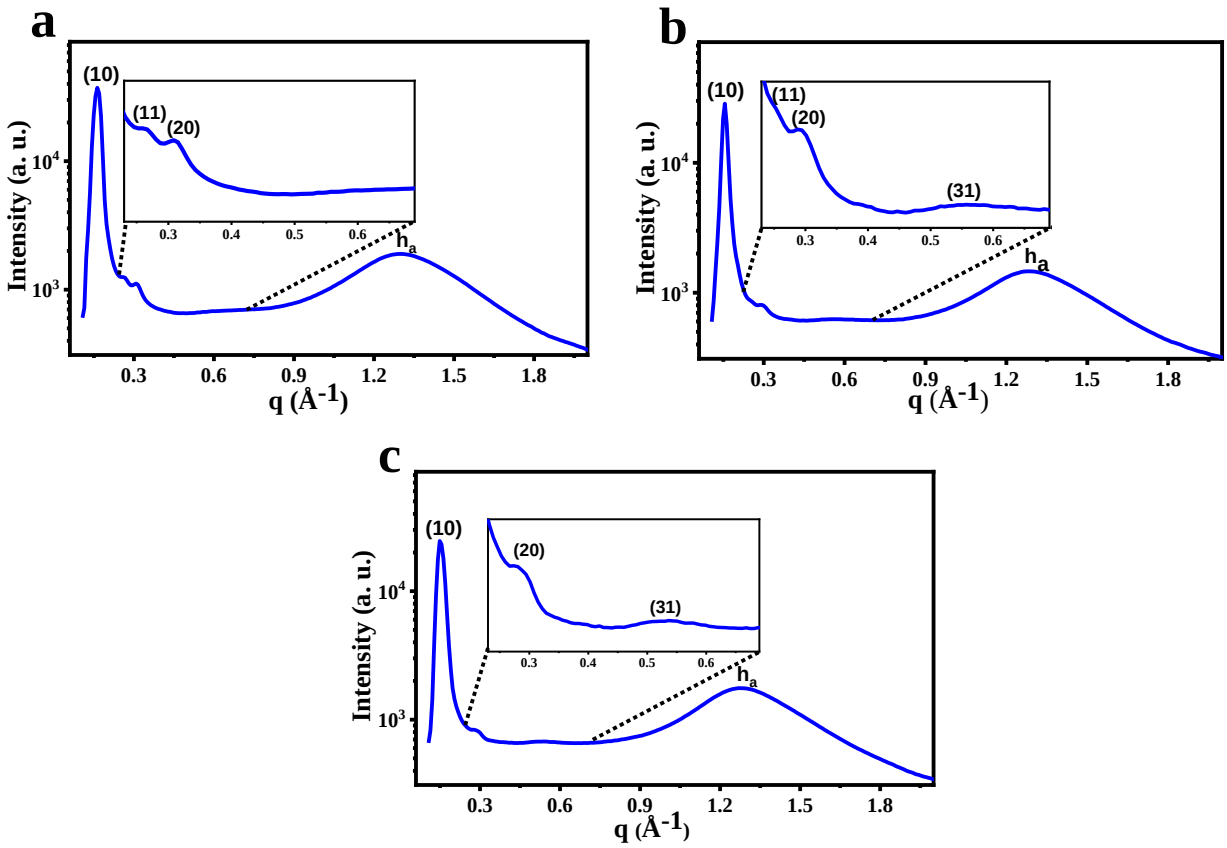

Figure S16. XRD pattern of compounds (a) **1a**, (b) **1b**, and (c) **1c** at 70 °C. The inset displays zoomed in view of the marked area (also Figure 1 in the main manuscript).

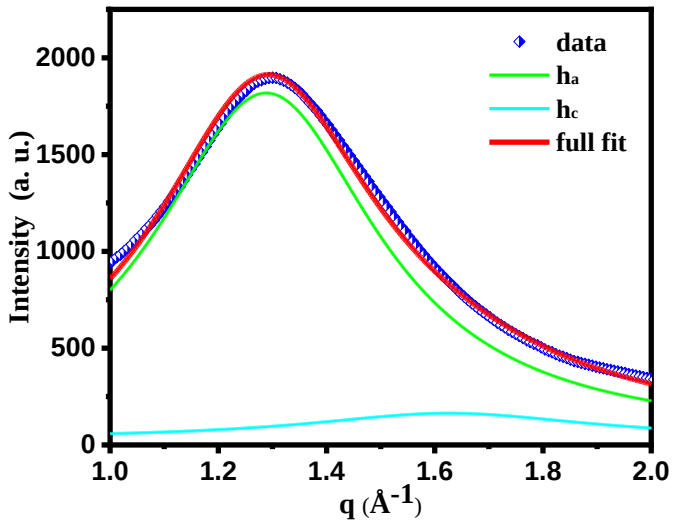

Figure S17. De-convolution of the wide-angle peak of the XRD pattern of compound **1a** at 70 °C. The half-filled diamond in blue shows the wide-angle data, and green, cyan, and red color curves show the h_a, h_c peaks, and full q fit of the wide-angle data.

Table S1. The observed and calculated *d*-spacings corresponding to the reflections from various planes of the 2D hexagonal lattice observed at 70 °C in compound **1a**.

Miller Indices *(hk)*	***d*-spacing Experimental d_{obs} (Å)**	***d*-spacing Calculated d_{cal} (Å)**	**Relative Intensity I (*hk*)**	**Multiplicity**	**Phase Φ (*hk*)**
10	39.99	39.99	100.00	6	0
11	23.21	23.04	3.32	6	π
20	19.98	20.00	2.99	6	0
h_a	4.84	Fluid alkyl chain			

The *d*-spacings were calculated by using the relation $\boldsymbol{d_{cal}} = \frac{\sqrt{3}\,a}{2\sqrt{h^2+h\,k+k^2}}$ where d_{cal} is calculated *d*-spacing, and *a is* the lattice parameter of the 2D hexagonal lattice. The calculated lattice parameter was *a* = 46.18 Å.

Table S2. The observed and calculated *d*-spacings corresponding to the reflections from various planes of the 2D hexagonal lattice observed at 70 °C in compound **1b**.

Miller Indices (*hk*)	***d*-spacing Experimental d_{obs} (Å)**	***d*-spacing Calculated d_{cal} (Å)**	**Relative Intensity I (*hk*)**	**Multiplicity**	**Phase Φ (*hk*)**
10	42.25	42.25	100.00	6	0
11	24.48	24.40	3.10	6	π
20	21.22	21.13	3.47	6	0
31	11.63	11.72	2.17	12	π
h_a	4.89	Fluid alkyl chain			

The *d*-spacings were calculated by using the relation $\boldsymbol{d_{cal}} = \frac{\sqrt{3}\,a}{2\sqrt{h^2+h\,k+k^2}}$ where d_{cal} is calculated *d*-spacing, and *a is* the lattice parameter of the 2D hexagonal lattice. The calculated lattice parameter was *a* = 48.79 Å.

Table S3. The observed and calculated *d*-spacings corresponding to the reflections from various planes of the 2D hexagonal lattice observed at 70 °C in compound **1c**.

Miller Indices (*hk*)	***d*-spacing Experimental d_{obs} (Å)**	***d*-spacing Calculated d_{cal} (Å)**	**Relative Intensity I (*hk*)**	**Multiplicity**	**Phase Φ (*hk*)**
10	42.69	42.69	100.00	6	0
20	21.46	21.34	3.34	6	0
31	11.87	11.84	2.74	12	π
h_a	4.93	Fluid alkyl chain			

The *d*-spacings were calculated by using the relation $\boldsymbol{d_{cal}} = \frac{\sqrt{3}\,a}{2\sqrt{h^2+h\,k+k^2}}$ where d_{cal} is calculated *d*-spacing, and *a is* the lattice parameter of the 2D hexagonal lattice. The calculated lattice parameter was *a* = 49.29 Å.

Electron Density Maps (EDMs):

EDMs were constructed using the peak indexes and intensities data. The procedure used was similar to that reported previously.[1]

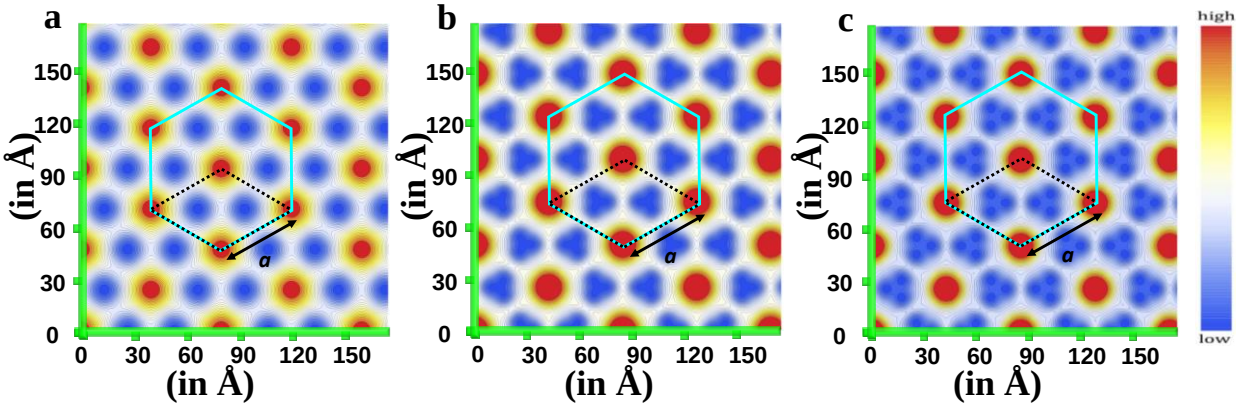

Figure S18: EDMs in the columnar hexagonal phase of compounds (a) **1a**, (b) **1b**, and (c) **1c** at 70 °C. Hexagon showed the conventional unit cell of the Col_h lattice, and there were three primitive unit cells within this conventional unit cell; a is the lattice parameter. Deep red indicates the highest electron density, and deep blue indicates the lowest.

8. Photophysical Studies

a. Absorption and emission in solution and thin-film state.

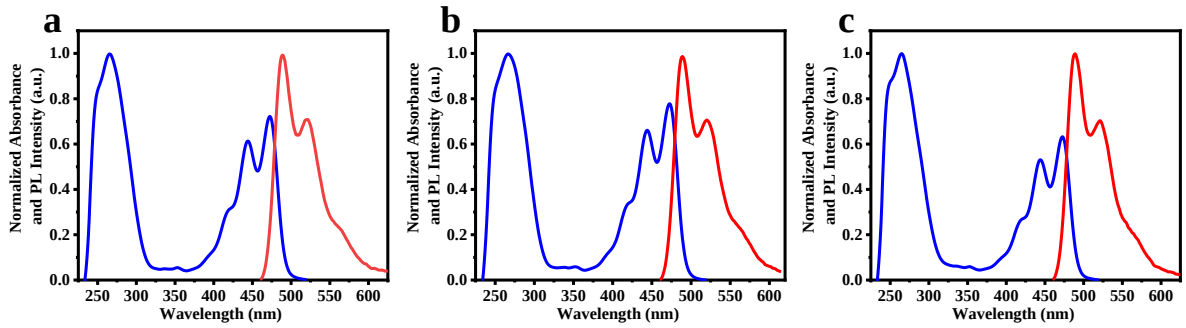

Figure S19. Absorption (shown in blue) and emission (shown in red) spectra of 10^{-5} M solution of compounds (a) **1a**, (b) **1b**, and (c) **1c** in THF.

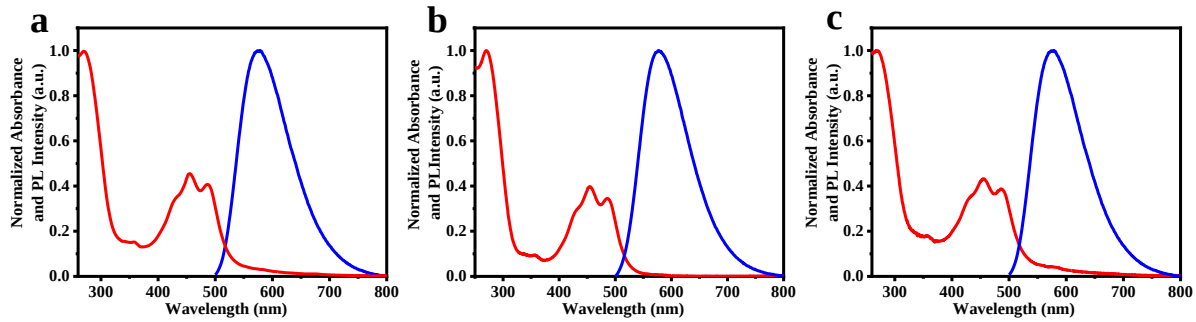

Figure S20. Absorption (shown in red) and emission (shown in blue) spectra of compounds (a) **1a**, (b) **1b**, and (c) **1c** in the thin-film.

b. Quantum yield measurements

The procedure used for quantum yield measurement is similar to the previous report[5] and is reproduced here for the reader's convenience.

Relative quantum yield was calculated using fluorescein (Φ_R = 0.79 in 0.1M NaOH) as the reference fluorophore.

The following equation was used for the calculation of quantum yield values:

$$\mathbf{\Phi_F} = \Phi_R \text{ x } \left(\frac{m_F}{m_R}\right) \text{ x } \left(\frac{\eta_F}{\eta_R}\right)^2$$

Where, Φ: fluorescence quantum yield, *m*: gradient of the plot of integrated fluorescence intensity against absorbance, η: refractive index of the solvent used (1.407 for THF and 1.33 for distilled water). Subscript R refers to the reference fluorophore, i.e., fluorescein in 0.1M aq. NaOH solution and subscript F refer to the fluorophore under investigation.

To minimize the re-absorption effects, the absorbance values were kept below 0.15.

After substituting all the values, the simplified equation was:

$$\mathbf{\Phi_F} = 0.79 \text{ x } \left(\frac{m_F}{m_R}\right) \text{ x } \left(\frac{1.407}{1.33}\right)^2$$

$$\mathbf{\Phi_F} = 0.88 \text{ x } \left(\frac{m_F}{m_R}\right)$$

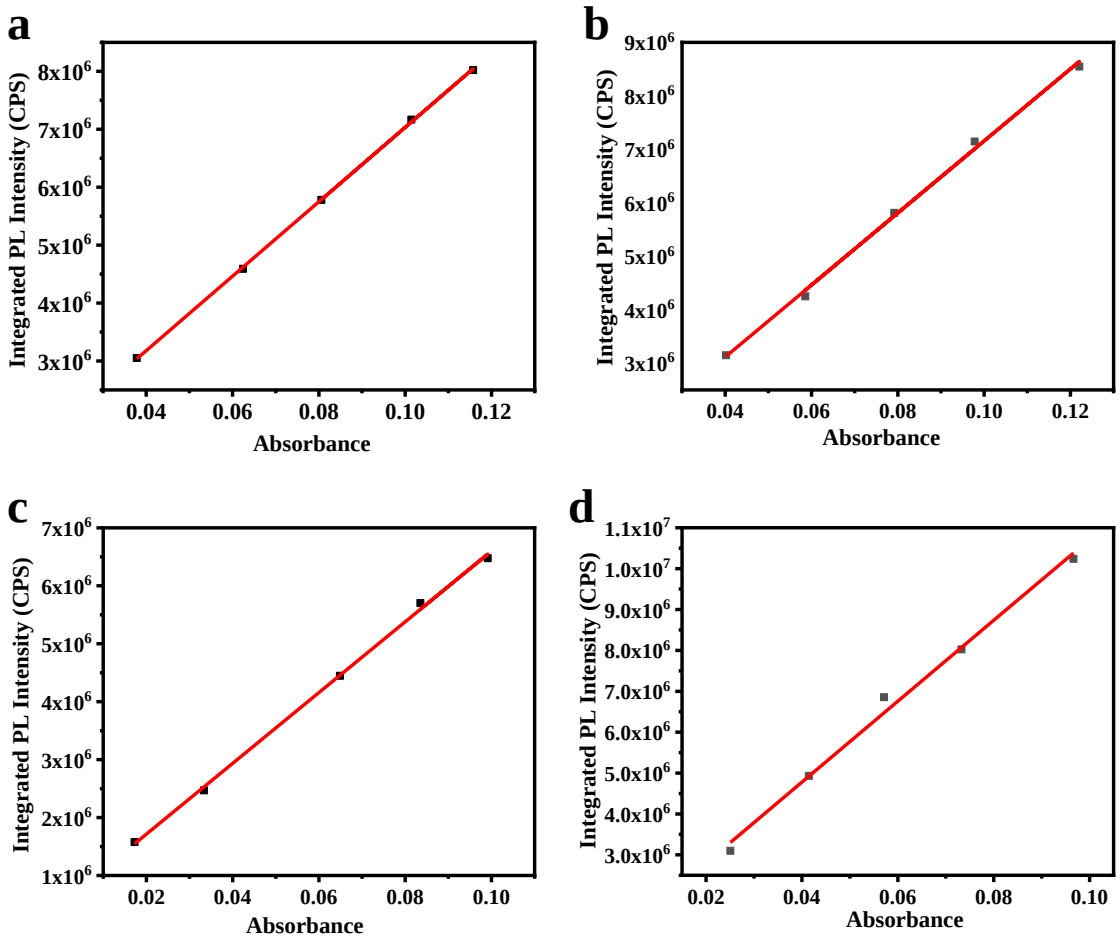

Figure S21. Plots of integrated photoluminescence intensity *vs.* absorbance of compounds (a) **1a**, (b) **1b**, and (c) **1c** in THF solution (λ_{exc} = 444 nm) and (d) Fluorescein in 0.1 M aq. NaOH solution (λ_{exc}= 491 nm).

Table S4. Quantum yield measurements [a, b]

Compound	m_F (*10^7)	m_R (*10^7)	Φ_F
1a	6.4273	9.89642	0.574
1b	6.73503	9.89642	0.602
1c	6.10827	9.89642	0.546

[a]Measured in THF. [b]Excited at absorption maxima.

Transient Photoluminescence (TRPL) and Low-Temperature Photoluminescence (LTPL) Studies

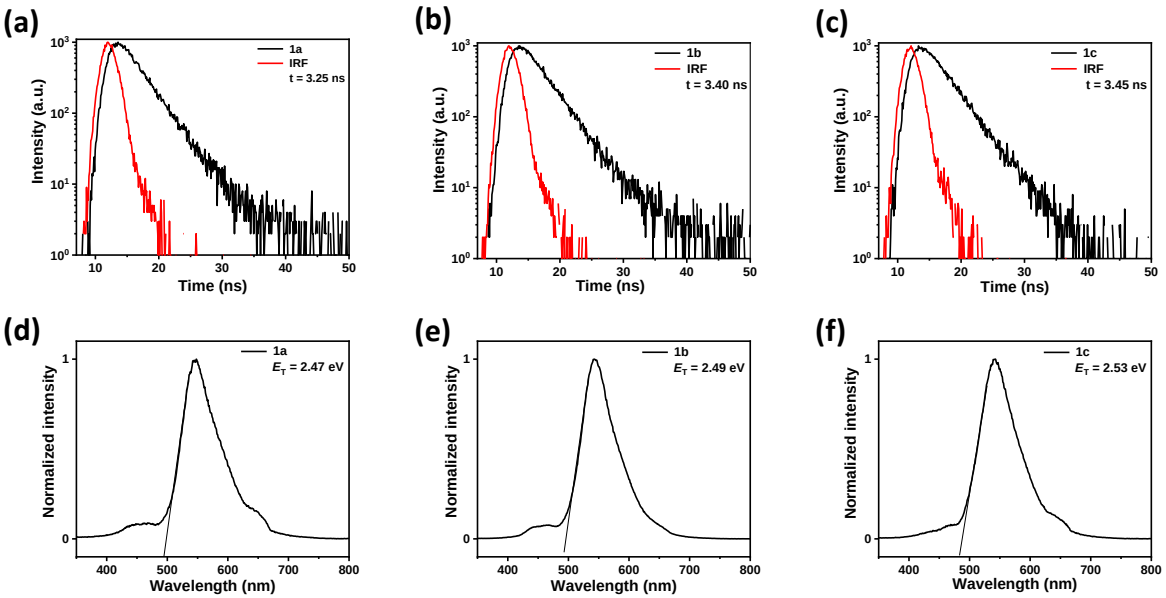

Figure S22. TRPL plot of (a) **1a**, (b) **1b**, and (c) **1c** showing decay time and LTPL of (d) **1a**, (e) **1b**, and (f) **1c** showing triplet energy.

9. Electrochemical Studies

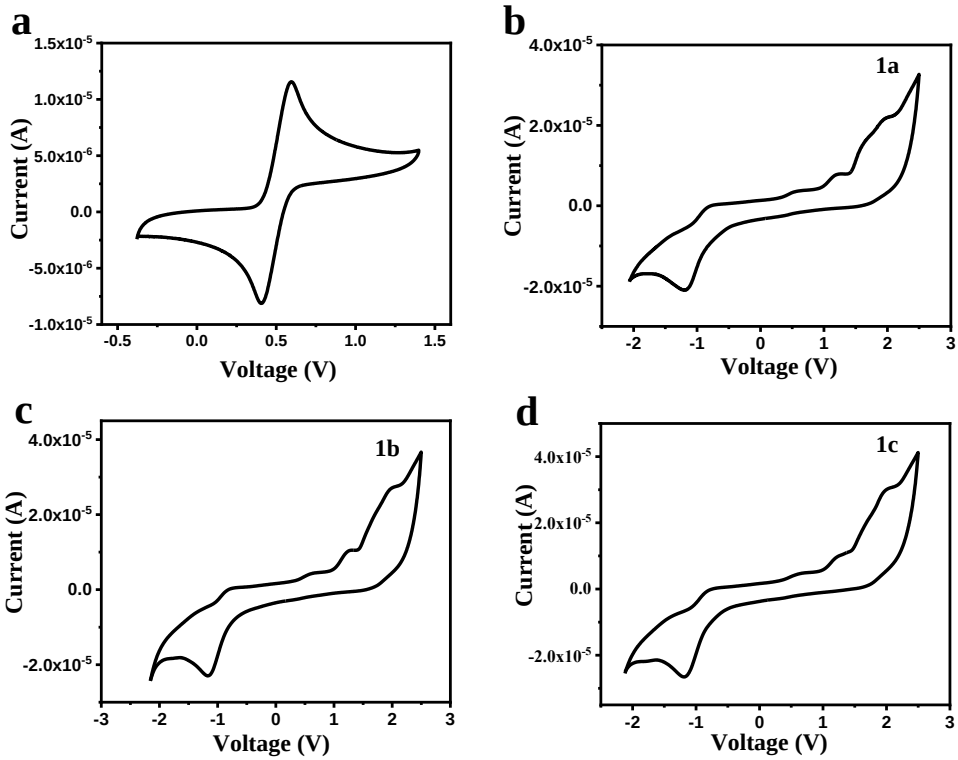

Figure S23. Cyclic voltammogram for (a) ferrocene (b) **1a**, (c) **1b**, and (d) **1c** at 0.05 Vs^{-1} scanning rate. Experimental conditions: reference electrode - $Ag/AgNO_3$, the counter electrode - platinum wire, working electrode - glassy carbon, and supporting electrolyte - 0.1 M TBAHFP.

Table S5. Electrochemical properties of compounds **1a-c** [a]

Compound	E_{HOMO}[b] (eV)	E_{LUMO}[c] (eV)	$\Delta E_{g,CV}$[d] (eV)	$\lambda_{UV\ onset}$[e] (nm)	$\Delta E_{g,UV}$[f] (eV)
1a	-5.73	-3.54	2.19	551	2.25
1b	-5.72	-3.52	2.20	549	2.26
1c	-5.78	-3.55	2.23	558	2.22

[a]Recorded in millimolar HPLC DCM solution. [b]Calculated using the formula $E_{HOMO} = -(4.8 - E_{1/2,Fc,Fc^+} + E_{oxd,onset})$ eV, where $E_{1/2,Fc/Fc^+} = 0.50$ V. [c]Obtained from the formula $E_{LUMO} = -(4.8 - E_{1/2,Fc,Fc^+} + E_{red,onset})$ eV. [d]Electrochemical band gap: $\Delta E_{g,CV} = E_{LUMO} - E_{HOMO}$. [e]Onset wavelength in thin-film absorption spectra. [f]Optical band gap: $\Delta E_{g,opt} = 1240/\lambda_{UV\ onset}$.

DFT Studies

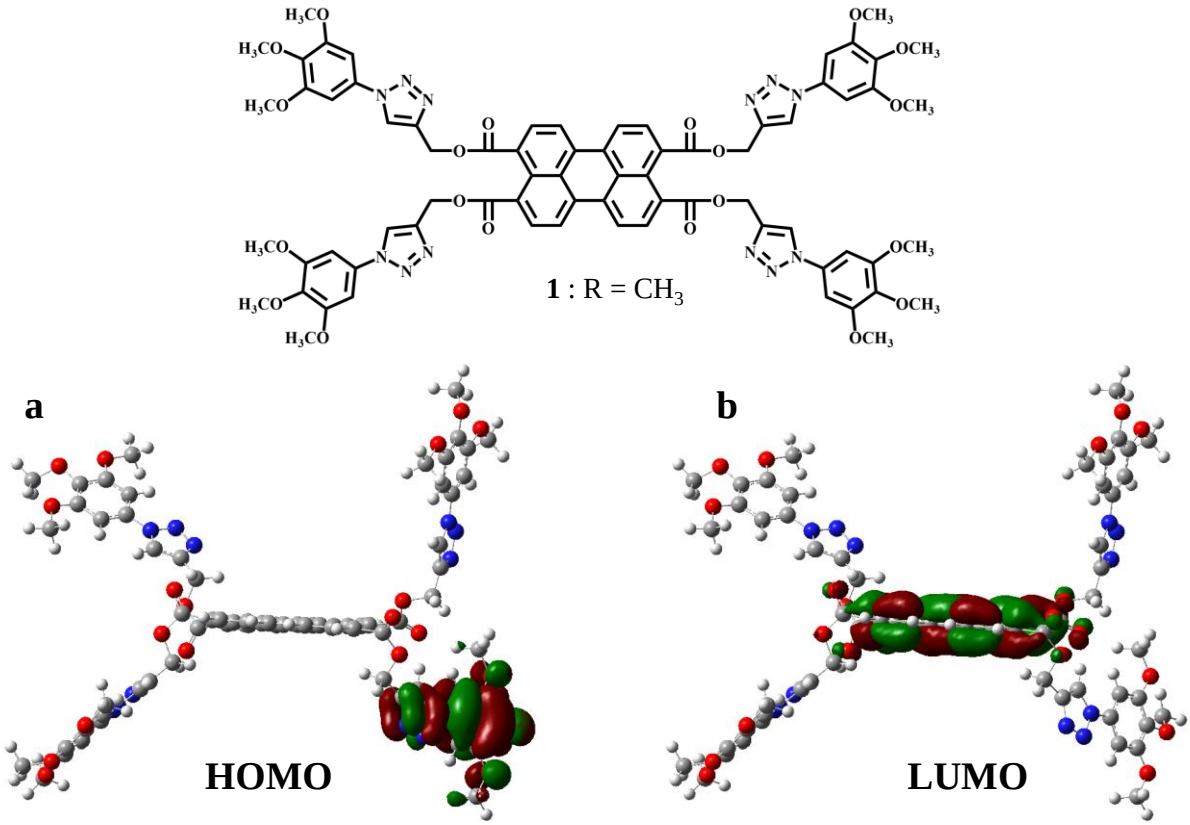

Figure S24. Electronic distribution of frontier molecular orbitals: (a) HOMO and (b) LUMO, for compound **1** (R = CH_3).

10. OLED Device Characteristics and Performance

Table S6. The electroluminescent properties of **1a-c** at a varying dopant concentration in the host m-MTDATA matrix

Emitter	Doping con. (wt%)	Driving Voltage (V)	PE_{max}/ CE_{max}/ EQE_{max} (lm W^{-1}/ cd A^{-1}/ %)	PE_{100}/ CE_{100}/ EQE_{100} (lm W^{-1}/ cd A^{-1}/ %)	PE_{1000}/ CE_{1000}/ EQE_{1000} (lm W^{-1}/ cd A^{-1}/ %)	CIE_{xy} coordinates at 100/1000 cd m^{-2}	Maxi. Lum. (cd m^{-2})
1a	**0.5**	2.5	10.7/10.3/3.1	6.2/7.0/2.2	1.2/2.2/0.7	(0.43,0.53)/(0.40, 0.53)	1994
	1	2.5	11.8/12.4/3.7	7.7/8.6/2.2	0.9/2.2/0.7	(0.43,0.53)/(0.41, 0.53)	1950
	3	3.0	8.5/6.7/2.0	7.2/6.4/1.9	1.4/2.3/0.6	(0.43, 0.54)/(0.40, 0.54)	1861
	100	6.6	-/-/-	-/-/-	-/-/-	-/-/-/	63
1b	**0.5**	2.5	11.4/9.1/2.9	8.7/8.3/2.3	1.5/2.5/0.8	(0.43,0.53)/(0.40, 0.53)	2067
	1	2.5	15.3/14.6/4.7	9.1/8.7/2.4	1.8/2.8/0.8	(0.42,0.54)/(0.40, 0.53)	2168
	3	2.5	13.7/10.9/3.2	7.9/8.8/2.5	1.4/2.4/0.7	(0.42,0.54)/(0.40, 0.53)	2038
	100	7.0	-/-/-	-/-/-	-/-/-	-/-/-	78
1c	**0.5**	2.5	9.8/7.8/2.1	7.6/7.2/2.0	1.7/2.8/0.8	(0.42,0.54)/(0.40, 0.53)	1896
	1	2.5	17.2/18.5/6.3	7.0/7.8/2.1	0.9/2.0/0.6	(0.42,0.53)/(0.40, 0.53)	2036
	3	2.5	14.4/11.4/4.2	8.8/8.4/2.3	1.5/2.9/0.8	(0.42,0.53)/(0.40, 0.53)	2164
	100	6.0	-/-/-	-/-/-	-/-/-	-/-/-	59

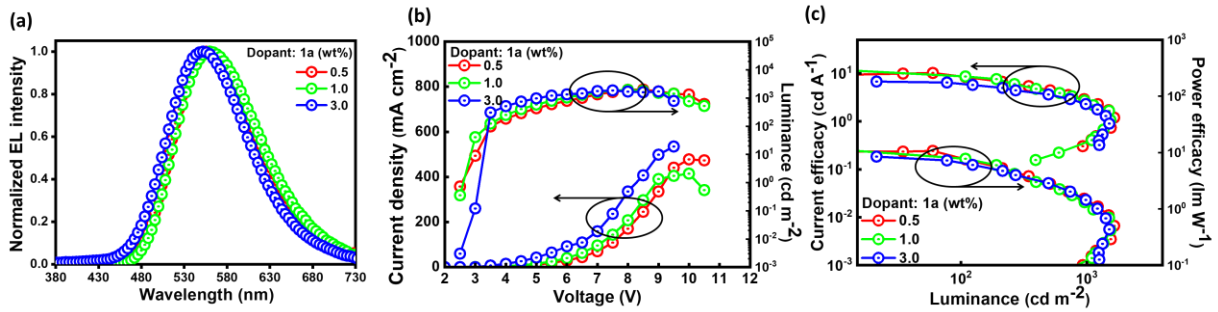

Figure S25. (a) EL spectra, (b) current density-voltage-luminance, and (c) current efficiency-luminance-power efficiency of the **1a** at different doping concentrations in the m-MTDATA host matrix.

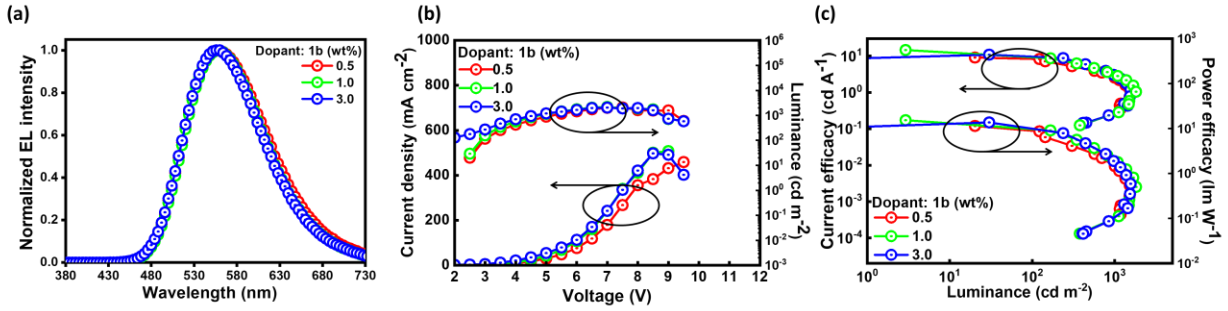

Figure S26. (a) EL spectra, (b) current density-voltage-luminance, and (c) current efficiency-luminance-power efficiency of the **1b** at different doping concentrations in the m-MTDATA host matrix.

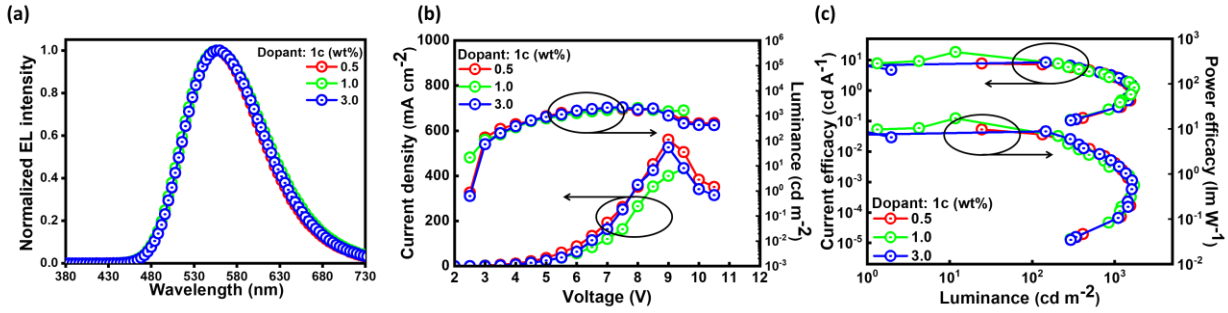

Figure S27. (a) EL spectra, (b) current density-voltage-luminance, and (c) current efficiency-luminance-power efficiency of the **1c** at different doping concentrations in the m-MTDATA host matrix.

Table S7. The electroluminescent properties of **1a-c** at a varying dopant concentration in the host CBP matrix

Emitter	Doping con. (wt%)	Driving Voltage (V)	PE_{max}/ CE_{max}/ EQE_{max} (lm W^{-1}/ cd A^{-1}/ %)	PE_{100}/ CE_{100}/ EQE_{100} (lm W^{-1}/ cd A^{-1}/ %)	PE_{1000}/ CE_{1000}/ EQE_{1000} (lm W^{-1}/ cd A^{-1}/ %)	CIE_{xy} coordinates at 100/1000 cd m^{-2}	Maxi. Lum. (cd m^{-2})
1a	**1**	5.3	5.0/9.7/5.8	5.0/9.7/5.8	1.5/3.3/1.3	(0.34, 0.48)/ (0.31, 0.39)	2403
	3	6.5	4.3/9.6/3.9	4.3/9.6/3.9	3.0/7.3/2.6	(0.40, 0.52)/ (0.39, 0.50)	4933
	5	6.6	2.4/5.9/2.3	2.4/5.4/2.3	2.4/5.9/2.2	(0.41, 0.51)/ (0.41, 0.51)	4790
	100	6.6	-/-/-	-/-/-	-/-/-	-/-/-/	63
1b	**1**	6.6	4.5/9.3/3.0	2.6/6.3/2.8	1.2/3.1/1.1	(0.38, 0.54)/ (0.34, 0.46)	2473
	3	7.5	3.8/9.1/4.1	3.8/9.1/4.1	2.7/6.8/2.5	(0.41, 0.52)/ (0.40, 0.52)	5018
	5	7.0	2.5/6.7/2.8	2.5/6.4/2.8	2.5/6.7/2.5	(0.43, 0.53)/ (0.42, 0.51)	3750
	100	7.0	-/-/-	-/-/-	-/-/-	-/-/-	78
1c	**1**	5.7	3.2/6.7/2.9	3.2/6.7/2.9	1.6/3.7/1.3	(0.34, 0.46)/ (0.33, 0.43)	2497
	3	6.1	3.1/6.9/2.8	3.1/6.9/2.8	2.0/4.9/1.7	(0.40, 0.51)/ (0.39, 0.49)	3410
	5	6.0	2.6/5.3/1.7	2.6/5.3/1.7	1.7/4.0/1.3	(0.41, 0.51)/ (0.40, 0.50)	2523
	100	6.0	-/-/-	-/-/-	-/-/-	-/-/-	59

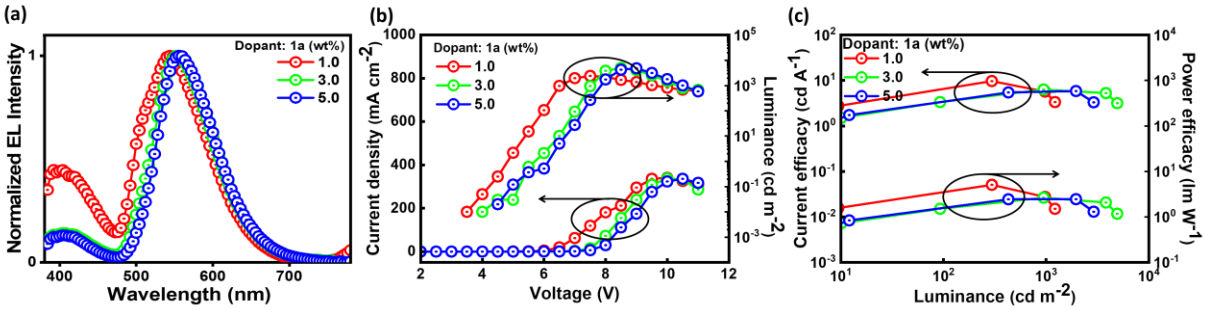

Figure S28. (a) EL spectra, (b) current density-voltage-luminance, and (c) current efficiency-luminance-power efficiency of the **1a** at different doping concentrations in the CBP host matrix.

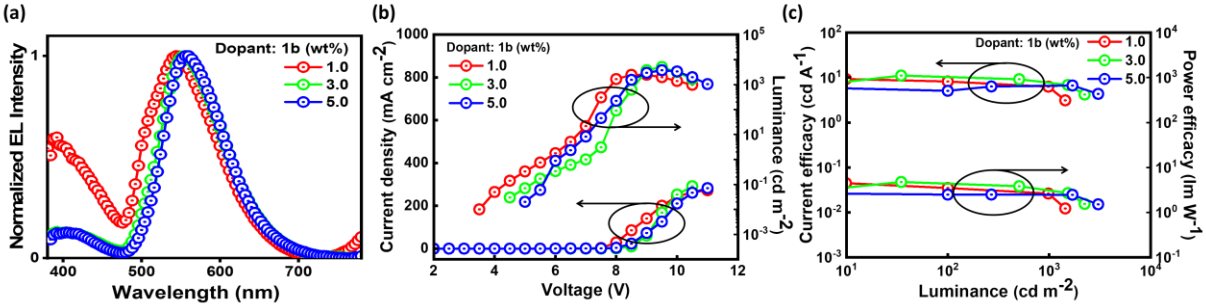

Figure S29. (a) EL spectra, (b) current density-voltage-luminance, and (c) current efficiency-luminance-power efficiency of the **1b** at different doping concentrations in the CBP host matrix.

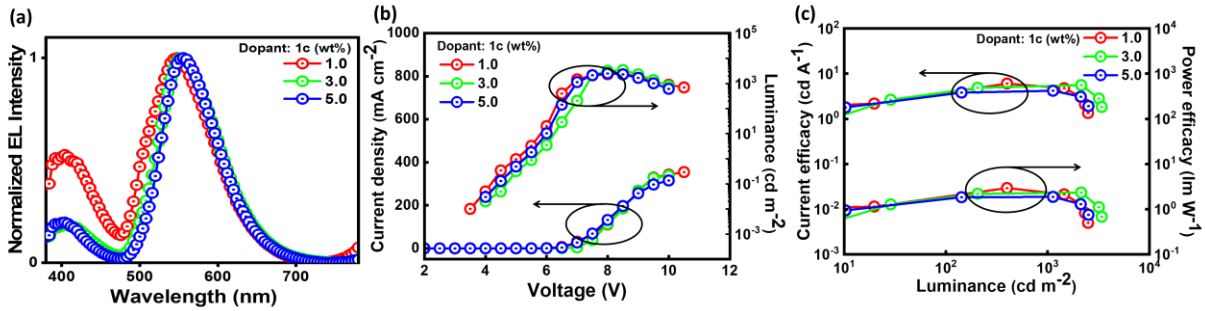

Figure S30. (a) EL spectra, (b) current density-voltage-luminance, and (c) current efficiency-luminance-power efficiency of the **1c** at different doping concentrations in the CBP host matrix.

11. References

1. S. Dhingra, I. Bala, J. De, S. P. Gupta, U. K. Pandey and S. K. Pal, *J. Mater. Chem. C*, 2021, **9**, 5628-5632
2. I. Bala, H. Kaur, M. Maity, R. A. K. Yadav, J. De, S. P. Gupta, J.-H. Jou, U. K. Pandey and S. K. Pal, *ACS Appl. Electron. Mater.*, 2022, **4**, 1163-1174.
3. I. Bala, S. P. Gupta, S. Kumar, H. Singh, J. De, N. Sharma, K. Kailasam and S. K. Pal, *Soft matter*, 2018, **14**, 6342-6352.
4. J. De, S. P. Gupta, S. S. Swayamprabha, D. K. Dubey, I. Bala, I. Sarkar, G. Dey, J.-H. Jou, S. Ghosh and S. K. Pal, *J. Phys. Chem. C*, 2018, **122**, 23659-23674.
5. I. Bala, N. Singh, R. A. K. Yadav, J. De, S. P. Gupta, D. P. Singh, D. K. Dubey, J.-H. Jou, R. Douali and S. K. Pal, *J. Mater. Chem. C*, 2020, **8**, 12485-12494.
6. J. Kim, S. Cho and B. K. Cho, *Chem. Eur. J.*, 2014, **20**, 12734-12739.
7. E. Aydin, B. Nisanci, M. Acar, A. Dastan, and Ö.A Bozdemir, *New J. Chem.*, 2015, **39**, 548-554.